ELSEVIER

Contents lists available at ScienceDirect

## Science of the Total Environment

journal homepage: www.elsevier.com/locate/scitotenv





## Hemispheric-scale heavy metal pollution from South American and Australian mining and metallurgy during the Common Era

Joseph R. McConnell<sup>a,\*</sup>, Nathan J. Chellman<sup>a</sup>, Sophia M. Wensman<sup>a</sup>, Andreas Plach<sup>b</sup>, Charles Stanish<sup>c</sup>, Pamela A. Santibáñez<sup>a</sup>, Sandra O. Brugger<sup>a</sup>, Sabine Eckhardt<sup>d</sup>, Johannes Freitag<sup>e</sup>, Sepp Kipfstuhl<sup>e</sup>, Andreas Stohl<sup>b</sup>

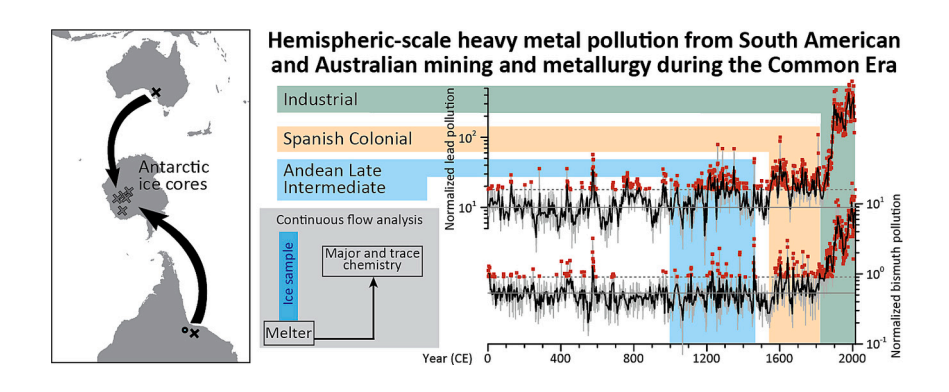
- <sup>a</sup> Division of Hydrologic Sciences, Desert Research Institute, Reno, NV 89512, USA
- <sup>b</sup> Department of Meteorology and Geophysics, University of Vienna, 1090 Vienna, Austria
- c Institute for the Advanced Study of Culture and the Environment, University of South Florida, Tampa, FL 33620, USA
- d Norwegian Institute for Air Research, N-2027 Kjeller, Norway
- <sup>e</sup> Alfred-Wegener-Institut Helmholtz-Zentrum für Polar- und Meeresforschung, 27570 Bremerhaven, Germany

#### HIGHLIGHTS

# • We report 2000-y records of Pb, Tl, Bi, and Cd fallout in five Antarctic ice cores.

- Volcanism was the source of 83 % to 99 % of pre-anthropogenic heavy metal fallout.
- Pb pollution attributed to Andean mining pervasive for much of the 2nd millennium.
- Order-of-magnitude increases in Pb, Bi, and Cd pollution since late 19th century.
- Atmospheric modeling suggests hemispheric-scale effects as a result.

#### GRAPHICAL ABSTRACT



#### ARTICLE INFO

Editor: Filip M.G. Tack

Keywords:
Metallurgy
Toxic heavy metals
Antarctica
Ice core
Common Era
Spanish Colonial

## ABSTRACT

Records from polar and alpine ice reflect past changes in background and industrial toxic heavy metal emissions. While Northern Hemisphere records have been used to evaluate environmental effects and linkages to historical events such as foreign conquests, plagues, economic downturns, and technological developments during the past three millennia, little is known about the magnitude and environmental effects of such emissions in the Southern Hemisphere or their historical linkages, especially prior to late 19th century industrialization. Here we used detailed measurements of the toxic heavy metals lead, cadmium, and thallium, as well as non-toxic bismuth, cerium, and sulfur in an array of five East Antarctic ice cores to investigate hemispheric-scale pollution during the Common Era. While thallium showed no anthropogenic increases, the other three metals increased by orders of magnitude in recent centuries after accounting for crustal and volcanic components. These first detailed records indicate that East Antarctic lead pollution started in the 13th century coincident with Late Intermediate Period metallurgy in the Andes and was pervasive during the Spanish Colonial period in parallel with large-scale exploitation of Andean silver and other ore deposits. Lead isotopic variations suggest that 19th-century increases in lead, cadmium, and bismuth resulted from Australian lead and Bolivian tin mining emissions, with 20th

<sup>\*</sup> Corresponding author at: Desert Research Institute, 2215 Raggio Parkway, Reno, NV 89512, USA. E-mail address: Joe.McConnell@dri.edu (J.R. McConnell).

century pollution largely the result of the latter. As in the Northern Hemisphere, variations in heavy metal pollution coincided with plagues, cultural and technological developments, as well as global economic and political events including the Great Depression and the World Wars. Estimated atmospheric heavy metal emissions from Spanish Colonial-era mining and smelting during the late 16th and early 17th century were comparable to estimated European emissions during the 1st-century apex of the Roman Empire, with atmospheric model simulations suggesting hemispheric-scale toxic heavy metal pollution during the past five centuries as a result.

#### 1. Introduction and background

Lead (Pb) and other low-boiling point heavy metals including bismuth (Bi), cadmium (Cd), and thallium (Tl) have three primary sources in remote environments: continental dust (Vallelonga et al., 2002), volcanism (Edmonds et al., 2018; Hinkley et al., 1999; Matsumoto and Hinkley, 2001; McConnell et al., 2017), and anthropogenic pollution from mining and metallurgy, fossil fuel combustion, and other industrial activities (Candelone et al., 1995; McConnell and Edwards, 2008; McConnell et al., 2002a; McConnell et al., 2014). All but Bi are highly toxic and potentially harmful to both human and ecosystem health. These metals are found in many precious and base metal geologic deposits so mining and metallurgy has resulted in heavy metal pollution for thousands of years even in some of Earth's most remote regions (Nriagu, 1983) as recorded by lake sediments (Bindler, 2006; Cooke and Bindler, 2015), peat bogs (Shotyk et al., 1998), and ice (Eichler et al., 2015; Hong et al., 1994; McConnell et al., 2018; McConnell et al., 2019; Uglietti et al., 2015; Wolff and Suttie, 1994). For example, detailed, year-by-year records of Pb pollution in a wide array of Arctic ice cores documented substantial changes in anthropogenic emissions during the past three millennia in response to plagues, wars, and technological advancements, starting with Greek and Roman-era mining and smelting of silver ores in the Mediterranean region (McConnell et al., 2018) and later European-wide metallurgy during the Middle Ages and Early Modern Period (McConnell et al., 2019). Heavy metal pollution from widespread combustion of fossil fuels-including the use of Pb as an additive for gasoline—resulted in a ~300-fold increase in Arctic Pb pollution during the early 1970s compared to near background levels at the early 6th-century start of the European Middle Ages (McConnell

Provenance of Pb pollution may be identified using isotopic fingerprinting techniques. Stable isotopes of Pb (204Pb, 206Pb, 207Pb, and <sup>208</sup>Pb) are not measurably fractionated during physicochemical processes so natural (e.g., volcanism) and anthropogenic (e.g., smelting, fossil fuel combustion) emissions retain the isotopic signature of their original source material. Because major sources of Pb have been isotopically characterized (Sangster et al., 2000), mixing models can be used to identify and quantify sources of Pb in environmental archives. As a result of the low concentrations of Pb in ice cores, previous studies have focused largely on the latter half of the 20th century during the apex of industrial emissions, and primarily in the Northern Hemisphere where Pb fluxes are higher (e.g., (Barbante et al., 2003; Liu et al., 2011; Rosman et al., 1994)). Pb isotopic ratios measured in ice cores from earlier periods have been used to identify and quantify the importance of British Isles coal burning during the First Industrial Revolution, the onset of Australian Pb ore smelting in Europe, and the rising importance of Chinese emissions following phase-out of North American and European leaded gasoline (Wensman et al., 2022).

Historical records and archaeological evidence (TePaske, 2010), corroborated by proxy pollution records from nearby ice (Eichler et al., 2015; Uglietti et al., 2015) and lake sediment cores (Cooke and Bindler, 2015), suggest that emissions from Andean silver, Pb, and other mining and smelting operations in the Altiplano region of modern Bolivia and Peru resulted in pronounced local contamination as early as the 1st millennium. The outsized influence of nearby sources, however, limits the use of these local archives for assessing the magnitude of overall

emissions and thus regional-scale human exposure to toxic metals and large-scale environmental impacts. While distal records from Antarctic ice cores located many thousands of kilometers away from low- and midlatitude emission sources offer the potential for much larger scale assessments, Pb pollution has been observed unambiguously in Antarctic snow and ice deposited only after the late 19th century (Planchon et al., 2003; Van de Velde et al., 2005; Wolff and Suttie, 1994), and not at all for Tl, Bi and Cd. Indeed, measurements in a wide array of shorter Antarctic ice cores spanning the past 400 years showed that Pb pollution since the late 19th century was pervasive over the continent (McConnell et al., 2014), with Pb isotopic studies (McConnell et al., 2014; Vallelonga et al., 2010; Vallelonga et al., 2002; Van de Velde et al., 2005) suggesting that large-scale Antarctic Pb pollution in the late 19th century could be attributed predominantly to Broken Hill mining and metallurgy in South Australia starting ~1889.

Identification and attribution of heavy metal pollution in Antarctic ice prior to the Industrial period, however, has been precluded by (1) low levels of anthropogenic fallout because continental Antarctic ice coring sites are located far from potential mid- and low-latitude emission sources, and (2) relatively high background variability from dust and especially volcanic fallout that masks anthropogenic contributions (Matsumoto and Hinkley, 2001). Dust levels in Antarctic ice are very low and only about 10 % of those in Arctic ice, so most of the background variability in heavy metals has been attributed to unspecified variations in quiescent volcanic emissions (Matsumoto and Hinkley, 2001; Vallelonga et al., 2002).

Here we used continuous measurements of Pb, Bi, Cd, Tl, cerium (Ce), and sulfur (S) in five East Antarctic ice cores, variations in discrete Pb isotopic ratios, as well as state-of-the-art FLEXPART atmospheric aerosol transport and deposition modeling, to evaluate hemispheric-scale heavy metal deposition in the Southern Hemisphere throughout the Common Era. After quantifying and subtracting background Pb, Bi, and Cd using Ce and Tl as proxies of dust and quiescent volcanism, respectively, we combined the measurements of the five cores to create and interpret the first comprehensive Common Era record of Antarctic heavy metal pollution.

#### 2. Methods

## 2.1. Ice core array

Detailed records of low-boiling-point heavy metal and other concentrations and depositional fluxes during the past 2000 years were developed in an array of five East Antarctic ice cores extending from 0° to 55°E and 75° to 82°S (Table 1, Fig. 1). All were collected without the use of drilling fluid (Liu et al., 2021). Contiguous, longitudinal samples were analyzed for a broad range of >30 elements and chemical species using the unique continuous ice core analytical system at the Desert Research Institute (DRI) (Criscitiello et al., 2021; McConnell et al., 2017; McConnell et al., 2002b; McConnell et al., 2014) and methods described previously (McConnell et al., 2017). Included were elemental measurements of sulfur, the low boiling point heavy metals Pb, Bi, Cd, and Tl, as well as the rock-forming rare-earth-element Ce. Every 2000-y record included ~6000 measurements of each element or nominally about three measurements per year on average. Smoothing within the flow system limited the effective depth resolution to ~0.02

m. Typical detection limits defined as three times the blank standard deviation were 0.005 to 0.010 pg/g for Cd, Tl, and Bi, and 0.030 to 0.060 pg/g for Ce and Pb.

The cores were volcanically synchronized (Sigl et al., 2014) (Supplementary Fig. 1) to the annual-layer-counted WAIS Divide ice core from West Antarctica on the well-established WD2014 chronology (Sigl et al., 2015) using distinct peaks in sulfur concentration. Except for the B40 core collected from a site with sufficiently high net snow accumulation to permit pseudo-annual layer counting within the volcanic constraints, we assumed that accumulation rates were constant between volcanic tie points. Absolute uncertainty in the WD2014 chronology during the Common Era generally is <3 years because it is based on annual layer counting constrained by numerous volcanic and other tie points, including short-lived cosmogenic nuclide events during the 1st millennium CE that were recorded both in ice and absolutely dated tree ring chronologies (Sigl et al., 2015). In addition, new cosmogenic nuclide measurements in WAIS Divide and B53 ice indicate an error of <2 years in the WD2014 chronology at the recently discovered cosmogenic nuclide event that occurred ~660 BCE (O'Hare et al., 2019). Following standard procedures, concentration measurements were multiplied by net accumulation rates (Table 1) to determine annual depositional fluxes. Because the synchronized ice core records show that long-term accumulation rates varied by <10 % during the Common Era, recent rates (19th and 20th century averages) were used except for the annually layer counted B40 record.

#### 2.2. Atmospheric aerosol transport and deposition modeling

As in other recent evaluations of anthropogenic aerosols measured in polar ice (McConnell et al., 2018; McConnell et al., 2021; McConnell et al., 2019), our interpretation was underpinned by FLEXPART (version 10.4) atmospheric aerosol transport and deposition model (Eckhardt et al., 2017; Pisso et al., 2019) simulations. Long-range atmospheric transport of pollutants is implicit because the East Antarctic ice core sites are located ~7000 to ~9000 km from potential Andean emission sites, and ~6200 to ~7600 km from potential Australian emission sites (McConnell et al., 2014; Vallelonga et al., 2002). To evaluate potential source regions, backward simulations (Eckhardt et al., 2017) were conducted for all five East Antarctic coring sites (Table 1), as well as for the more proximal, high-elevation Quelccaya North Dome (QND; 13.93°S, 70.83°W) ice coring site – one of the few Andean sites for which well-dated, high-time-resolution heavy metal, Ce, and other records are available (Uglietti et al., 2015). Forward simulations also were conducted for selected potential heavy metal emission sites to assess spatial patterns of pollution fallout around the Southern Hemisphere with emission magnitudes estimated from deposition rates measured in the ice core array and emission sensitivities from the backward simulations (McConnell et al., 2021). Sites included well-recognized mining and metallurgy sources near Port Pirie, Australia (33.2°S, 138.0°E) (McConnell et al., 2014) and Potosí, Bolivia (19.6°S, 65.8°W) (Brown, 2012). To approximate potential Pb and Bi emissions from the more widely distributed Bolivian tin mining region, we averaged forward simulation results from Potosí, Tiwanaku, Bolivia (16.6°S, 68.7°W), and Puno Bay, Peru (15.9°S, 70.0°E).

Sophisticated atmospheric aerosol models such as FLEXPART require detailed meteorological fields. These are not available prior to the 20th

prior to the 1980s by the lack of satellite observations. Therefore, as in related studies of anthropogenic aerosols (Legrand et al., 2022; McConnell et al., 2018; McConnell et al., 2021; McConnell et al., 2019), we assumed that long-range atmospheric transport was relatively stable during the Common Era and used the 1980 to 2019 ERA5 reanalysis fields produced by European Centre for Medium Range Weather Forecasts (ECMWF) (Hersbach et al., 2020) at 0.5° by 0.5° spatial and 1hourly temporal resolution with 137 vertical layers representing the atmosphere from the surface to a height of 80 km. Because the mismatch of model and actual topography in mountainous regions is still significant at a 0.5° resolution (i.e., parts of the Andes are too low in the model which results in an overestimation of wet deposition), we calculated the wet deposition at the (higher) actual Andean site altitude. Long-range atmospheric transport from potential mid-latitude source regions means that there are relatively small differences in emission sensitivities between the five East Antarctic ice core sites (McConnell et al., 2021) so average 1980 to 2019 1 µm dust emissions sensitivity fields for the individual sites in the East Antarctic ice core array were log-averaged to determine an array-average field (Supplementary Fig. 2).

century and atmospheric reanalysis quality over Antarctica is limited

#### 2.3. Lead isotopic measurements and isotopic mixing model simulations

Lead isotopic ratios were measured in available discrete B54 meltwater samples routinely collected during the continuous measurement campaign. Reconstituted acidified meltwater samples were measured on an Element2 HR-ICP-MS (Thermo) located in a class-100 clean room at DRI. Samples were introduced into the HR-ICP-MS using an Apex IR inlet system fitted with a PFA MicroFlow nebulizer (Elemental Scientific) and N<sub>2</sub> as the additional gas. Aside from instrumentation differences, sample preparation and measurement protocols (e.g., sample-standard bracketing, reference material analysis) followed established methods for analyzing Pb isotopes at very low-level concentrations typical of polar ice (Wensman et al., 2022). National Institute of Standards and Technologies (NIST, USA) SRM 981 natural Pb (isotopic) standard was used to bracket each sample during the measurements and to monitor instrument drift and normalization of all measured Pb isotopic ratios. Nine successive runs of NBS 981 were included at the start of each analytical session and concluded with an additional five successive runs. Procedural blanks contributed an estimated average of 0.02  $\pm$  0.01 % of the sample Pb signal. Measured reference materials (BCR-2 Columbia River Basalt, AGV-1 Guano Valley Andesite, and NIST 1643f Trace Elements in Water) differed from published values (Weis et al., 2006: Wensman et al., 2022) by an average of 0.2 % (<sup>206</sup>Pb/<sup>207</sup>Pb) and 0.1 % (<sup>208</sup>Pb/<sup>207</sup>Pb). Although the B54 samples were measured on an Element 2, uncertainties were  $\sim 0.2$  % (RSD) for  $^{206}\text{Pb}/^{207}\text{Pb}$  and  $^{208}\text{Pb}/^{207}\text{Pb}$ ratios and comparable to previous Pb isotopic results using an AttoM HR-ICP-MS (Nu Instruments) (Wensman et al., 2022).

We used the Bayesian isotopic mixing model MixSIAR (version 3.1.12) (Stock et al., 2018) to apportion sources of late 19th to early 20th century Pb pollution in Antarctica based on the B54 measurements and previously reported Pb isotopic measurements from two Antarctic sites: Law Dome (66.7°S, 113°E) (Vallelonga et al., 2002), and Coats Land (Site A: 77.6°S, 25.4°W; Site B. 77.3°S, 18.1°W) (Planchon et al., 2003). MixSIAR was chosen over a simple linear mixing model because it accounts for source heterogeneity and measurement error (Stock et al.,

Location and other details for Antarctic ice cores.

Ice core Site	Latitude (deg N)	Longitude (deg E)	Elevation (m)	Recent snowfall (kg/m²/y)	Year analyzed	References
						Chronology
B40	-75	0.1	2891	68	2013	McConnell et al., 2021
B53	-76.8	31.9	3729	29	2017	McConnell et al., 2021
B54	-79	30	3470	30	2019/2021	This study
NUS07_7	-82.1	54.9	3725	30	2018	McConnell et al., 2021
NUS07_5	-78.7	35.6	3619	24	2009	Sigl et al., 2015

2018) and has been successfully applied to the stable Pb isotopic system (Longman et al., 2018). The end-member isotopic compositions were defined using Australian, Andean, and Mexican ores (Sangster et al., 2000), and volcanic island basalts from Bouvet and Easter Island (Sun, 1980). Because of similarities in the isotopic compositions of the volcanic island basalts and Andean ores, these source signatures were averaged ( $^{206}$ Pb/ $^{207}$ Pb =  $1.21 \pm 0.02$ ,  $^{208}$ Pb/ $^{207}$ Pb =  $2.48 \pm 0.01$ ). Prior to MixSIAR analysis, the nbPb isotopic ratios were calculated using the likely background isotopic ratios for each core. For Law Dome, we assumed constant background Pb isotopic ratios of 1.124 and 2.484 for  $^{206}$ Pb/ $^{207}$ Pb and  $^{208}$ Pb/ $^{207}$ Pb, respectively, and a background Pb concentration of 0.35 pg/g based on average values for samples from 4500 BCE to 1729 CE (Vallelonga et al., 2002). For Coats Land, we used background Pb isotopic ratios of 1.196 and 2.469 for  $^{206}$ Pb/ $^{207}$ Pb and

<sup>208</sup>Pb/<sup>207</sup>Pb, respectively, and a Pb concentration of 0.167 pg/g estimated samples with the lowest enrichment factor (EF) from 1846 to 1857 CE (Planchon et al., 2003). For the B54 samples, we used background Pb isotopic ratios of 1.200 for <sup>206</sup>Pb/<sup>207</sup>Pb and 2.472 for <sup>208</sup>Pb/<sup>207</sup>Pb, and variable background Pb concentrations (1.35–1.82 pg/g) calculated as described in Section 3.2.

#### 3. Results and discussion

#### 3.1. Comparisons to previous measurements

Concentrations from the continuous measurements in the East Antarctic array (Supplementary Fig. 3) were similar to the few previously reported discrete measurements in Antarctic Holocene snow and ice,

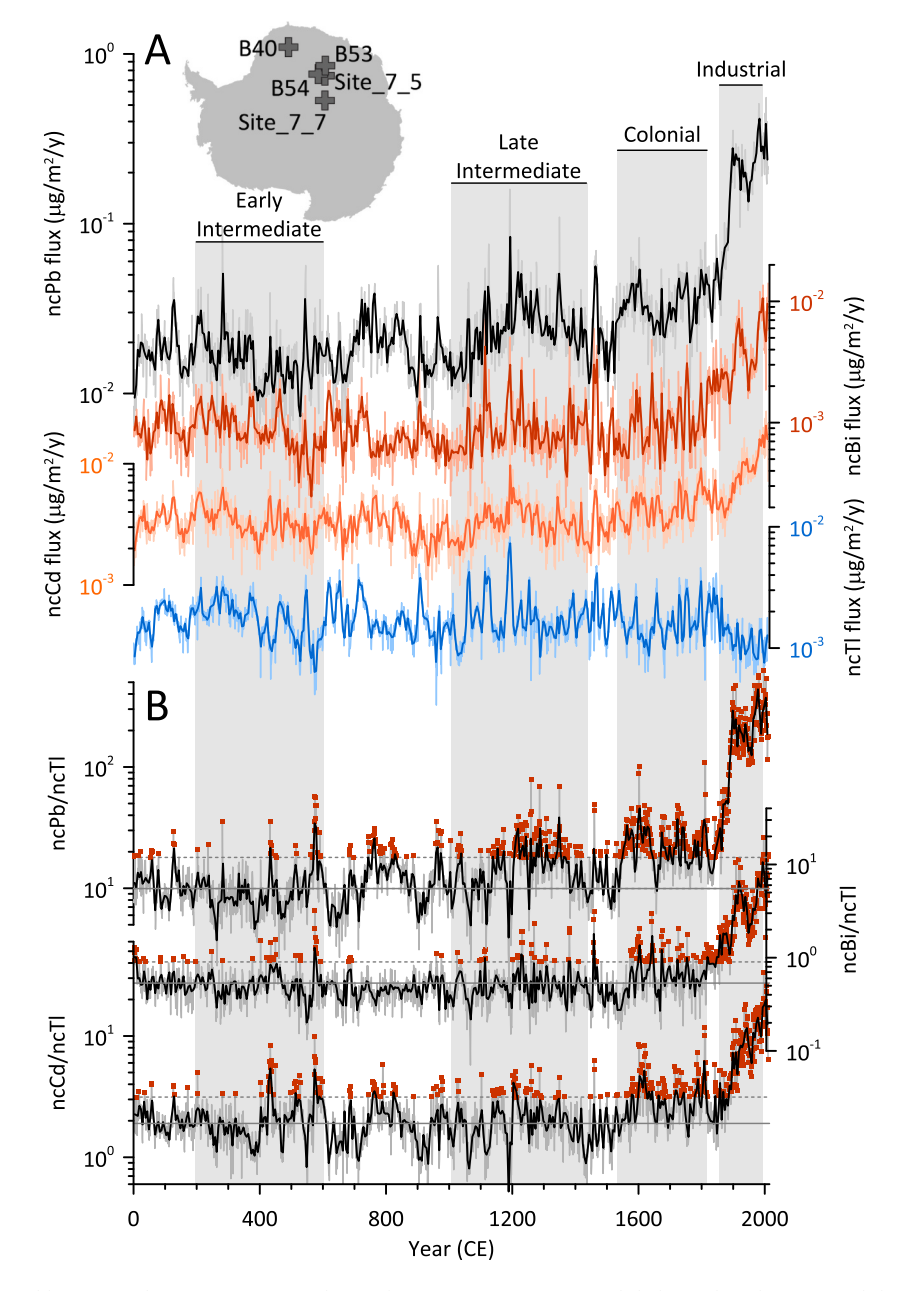


Fig. 1. Deposition of non-crustal heavy metals in East Antarctica during the Common Era. (a) Annual (light) and 5-y log-averaged (heavy) composite fluxes of non-crustal lead (Pb), bismuth (Bi), cadmium (Cd), and thallium (Tl) from an array of five East Antarctic ice cores (inset). (b) Annual (light) and 5-y log-averaged ratios of non-crustal Pb, Bi, and Cd to non-crustal Tl, with non-crustal Tl used as an indicator of fallout from quiescent volcanism. Solid horizontal lines show the mean ratio during a pre-anthropogenic calibration period from 1 to 400 CE. Dotted horizontal lines show 2 s.d. above the annual ratio mean used as the threshold to identify periods likely influenced by anthropogenic emissions (red filled squares). The 2 s.d. criterion means that ~2.5 % of annual values will exceed the threshold even without anthropogenic contributions. Shading shows major historical periods in South American history.

with very low concentrations of Tl, Bi, and Cd in pre-Colonial ice averaging ~0.1 pg/g (range 0.01 to 0.52 pg/g); Pb and Ce concentrations were about an order of magnitude higher. Previous archaeological studies (Cooke et al., 2008), as well as measurements in Andean ice (Eichler et al., 2015; Uglietti et al., 2015) and lake sediment cores (Cooke and Bindler, 2015) suggest that Southern Hemisphere anthropogenic heavy metal emissions were negligible during the early 1st millennium. Therefore, we used measurements from 1 to 400 CE as a calibration period assuming no anthropogenic inputs (i.e., only dust and volcanic sources). Annual average and geometric mean Tl concentrations during this calibration period ranged from 0.073 ( $\pm$  0.001 SE) and 0.069 pg/g in the B53 core, respectively, to 0.077 ( $\pm$  0.001 SE) and 0.073 pg/g in the B54 core. These compare to the very few reported measurements of Tl in Antarctic ice of 0.06 (range 0.02 to 0.12) pg/g in discrete samples from interglacial periods in the EPICA Dome C core (Hur et al., 2013) and 1956 to 2008 concentrations of 0.07 pg/g (range 0.03 to 0.18 pg/g) in a snowpit from nearby Dome Fuji (Hong et al., 2012).

Annual average and geometric mean Pb concentrations during the 400-y calibration period ranged from 0.674 ( $\pm$  0.026 SE) and 0.568 pg/g in the B40 core, respectively, to 1.176 ( $\pm$  0.028 SE) and 1.073 pg/g in the NUS07\_7 core. These compare to 0.21 (range 0.2 to 0.3) pg/g in discrete preindustrial Holocene samples in the EPICA Dome C core (Vallelonga et al., 2010). Finally, annual average and geometric mean Ce concentrations ranged from 0.600 ( $\pm$  0.019 SE) and 0.524 pg/g in the B53 core, respectively, to 0.723 ( $\pm$  0.025 SE) and 0.591 pg/g reported in discrete Holocene samples from the EPICA Dome C core (Gabrielli et al., 2010).

Lead isotopic ratios measured in B54 are similar to those observed in Law Dome and Coats Land (Fig. 5) beginning in the late 19th century, although with substantially less variability that likely is the result of the much lower temporal resolution of the B54 samples. Isotopic ratios during periods prior to the late 19th century show substantial site-to-site differences in Pb isotopic composition (e.g.,  $^{206} {\rm Pb/}^{207} {\rm Pb} = 1.18$  for B54, and  $^{206} {\rm Pb/}^{207} {\rm Pb} = 1.24$  for Law Dome in  $\sim \! 1600$ ). Such differences in isotopic ratios have been observed previously and attributed to variations in crustal rock, soil dust, and volcanism around the mid- and high-latitude regions of the Southern Hemisphere (Vallelonga et al., 2002).

## 3.2. Non-crustal heavy metal fluxes

Very long-range atmospheric transport means the anthropogenic contributions in Antarctic ice are small and there is substantial overlap in the FLEXPART-simulated potential industrial source regions for these coring sites located in the mid latitudes. Because of the relatively high uncertainties for such long-range transport, as well as glaciological noise at the ice core sites (most from very low snowfall sites where glaciological noise is especially pronounced), we opted to reduce uncertainties by combining the heavy metal records (Fig. 1) and the emission sensitivity fields (Supplementary Fig. 2) into Common Era composites.

Although limited to a few measurements of discrete samples, previous studies (Hinkley et al., 1999) have attributed background Pb and other heavy metals measured in preindustrial Antarctic ice to continental dust and volcanic fallout, with the latter being the substantially greater source. To identify and quantify anthropogenic Pb, Bi, and Cd, therefore, it is necessary to have independent indicators of dust and volcanic fallout measured in the same ice. As in prior studies (McConnell et al., 2018; McConnell et al., 2014), here we used exactly co-registered measurements of the rock-forming rare-earth-element Ce as an indicator of crustal dust. Unlike some other indicators of dust such as calcium or barium, there are few, if any, contributions of Ce or other rare earth elements from ocean or non-explosive volcanic sources. In addition, Ce is the most abundant rare earth element. We calculated crustal components of Tl, Pb, Bi, and Cd using mean sediment abundances (Bowen, 1979) and measured Ce concentrations, with Ce concentrations scaled

by 1.6 to account for under recovery in the continuous measurements (McConnell et al., 2007). These were subtracted from the measured total concentrations to yield non-crustal (e.g., ncPb) components.

Enrichments relative to Ce indicate that  ${\sim}89~\%$  of Pb,  ${\sim}95~\%$  of Bi,  ${\sim}99~\%$  of Cd, and  ${\sim}94~\%$  of Tl were from non-crustal sources during the 1 to 400 CE calibration period. Deposition of ncPb increased 15-fold from  ${\sim}0.02~\mu g/m^2/y$  during the 400-y calibration period to  ${\sim}0.30~\mu g/m^2/y$  during the 20th century (Fig. 1). Fluxes of ncBi and ncCd also increased by an order-of-magnitude or more, while ncTl fluxes showed no trend and generally lower levels during the Industrial Period suggesting little or no contributions from anthropogenic emissions throughout the Common Era. Note that 19th- and 20th-century anthropogenic increases in Tl observed in Arctic ice have been attributed primarily to fossil fuel combustion rather than mining or metallurgy (McConnell and Edwards, 2008).

Annual and five-year averaged nc composite values during the 400-y calibration period all were highly and significantly (p < 0.0001) correlated (Table 2), with 18 to 58 % of the variability common between fiveyear averaged ncTl, ncPb, ncBi, and ncCd. Given that Tl has been shown to be emitted from quiescent volcanism (Hinkley et al., 1999; Matsumoto and Hinkley, 2001; McConnell et al., 2017), the close relationship of ncTl to ncPb, ncBi, and ncCd is consistent with common quiescent volcanic aerosol sources, as well as similar atmospheric (probably tropospheric) transport and deposition processes (Mason et al., 2022). Following standard procedures, non-sea-salt sulfur (nssS) was calculated from total S using exactly co-registered measurements of sodium and calcium, as well as elemental ratios in mean sea water and sediment (Bowen, 1979). Increases in ncTl and the other heavy metals rarely, if ever, coincided in the ice records with spikes in nssS associated with well-known explosive tropical eruptions (Supplementary Fig. 1). Sulfur fallout from such large tropical events generally results from oxidation of sulfur dioxide gas to sulfate aerosol and long-range transport in the stratosphere and so is distinct from fallout transported via the troposphere. Therefore, we used the ratio of ncTl flux to ncPb, ncBi, and ncCd fluxes to correct for quiescent volcanic inputs and thereby initially identified years of possible anthropogenic fallout in East Antarctica. Only years in which the metal to ncTl ratio exceeded the 2 s.d. background variability during the 400-y calibration period were identified as polluted. Results (Fig. 1) suggest that sustained periods of Pb pollution in East Antarctica occurred from ~1200 to ~1380 during the Late Intermediate Period in the Andes, ~1550 to ~1820 during the Colonial Period, and ~ 1850 to present corresponding to the modern Industrial period. Although short periods of Bi and Cd pollution occurred in the 17th and 18th centuries, sustained increases did not occur until the 19th century, mostly after ~1820 and ~ 1890, respectively. Although ncPb, ncBi, and ncCd all were markedly higher during the Industrial period, lower ncTl deposition after ~1850 suggests decreased quiescent volcanic emissions, thereby enhancing recent metal to ncTl ratios (Fig. 1).

Table 2
Correlations (Pearson's r) between non-crustal heavy metal fluxes.

	ncTl	ncPb	ncBi	ncCd			
0-400 CE, Annual							
ncTl	1.00	0.32	0.52	0.45			
ncPb		1.00	0.43	0.65			
ncBi			1.00	0.47			
ncCd				1.00			
0-400 CE, 5-yr							
ncTl	1.00	0.43	0.68	0.58			
ncPb		1.00	0.49	0.76			
ncBi			1.00	0.55			
ncCd				1.00			

#### 3.3. Non-background heavy metal fluxes

The East Antarctic records reported here show no evidence of anthropogenic Tl fallout during the past 2000 years (Fig. 1) so we used linear relationships between ncTl and ncPb, ncBi, and ncCd during the 400-y calibration period together with ncTl fluxes throughout the Common Era to estimate fallout from quiescent volcanism. These estimated volcanic contributions were subtracted from the non-crustal values to yield non-background (e.g., nbPb) concentrations and fluxes. Note that because nssS in Antarctic ice has multiple sources including marine biogenic emissions and both explosive and quiescent volcanic emissions, it is not suitable as a quantitative indicator of volcanic fallout. We similarly used Tl to calculate nbPb, nbBi, and nbCd fluxes in the Andes for the previously published QND ice core record (Uglietti et al., 2015), with effective ratios of Pb, Bi, and Cd to Tl in volcanic fallout determined during a 300-y calibration period from 1250 to 1550 when heavy metal concentrations in the QND record were low and so unlikely to have been influenced significantly by nearby anthropogenic emissions (Uglietti et al., 2015).

We assessed the likelihood that non-background heavy metal deposition was unrelated to natural sources—and therefore most likely a result of pollution—by comparing to the variability in non-background fluxes during the 400-y calibration period. We calculated the probability that non-background fluxes exceeded the 2 s.d. variability during the calibration period using 3- to 21-y averaging windows (Fig. 2; Supplementary Fig. 4) because we expect anthropogenic fluxes to be more persistent than volcanic emissions (e.g., from the discovery and decadeslong exploitation of specific mining districts such as Potosí). Except for Pb pollution between  $\sim\!1200$  to  $\sim\!1380$  during the Late Intermediate Period in the Andes, the ice records indicate little or no sustained heavy metal pollution in East Antarctica prior to European colonization of South America.

#### 3.4. Late Intermediate Period: 1000 to 1476 CE

The Late Intermediate Period was a time of political fragmentation in the Andean highlands. Nevertheless, the Chimú (circa 900 to ~1470 CE) emerged as a major urban-based imperial state on the north coast. The workshops in the capital city of Chan Chan consumed enormous quantities of silver and other metals and would have stimulated a high demand throughout the central Andes. Although it is not possible to identify specific Pb emission sources during this period, archaeological evidence from Puno Bay in modern Peru indicates that silver mining. smelting, and cupellation began as early as the 1st century in the southern Lake Titicaca region of the Altiplano and continued through the Spanish Conquest (Schultze et al., 2009). In addition, proximal lake sediment records from the Potosí region (Cooke et al., 2008) indicate that atmospheric Pb emissions began in the early 12th century and reached a Late Intermediate Period maximum in the 13th century consistent with the East Antarctic ice records (Supplementary Fig. 5). If the bulk of East Antarctic pollution originated from the central Andean highlands, we estimate 1210 to 1290 average Pb emissions of  $\sim$ 1.2 kt/y based on FLEXPART-simulated emission sensitivity of 0.458 ( $\mu g/m^2/y$ )/ (kg/s) at the East Antarctic array and nbPb deposition of 0.017  $\mu$ g/m<sup>2</sup>/y during this period.

#### 3.5. Colonial Period: Early 1530s to early 1820s

Pervasive East Antarctic Pb pollution began soon after the 1532 CE Spanish Conquest of South America and persisted for the most part to independence in the early 1820s (Fig. 2). The first period extended from  $\sim\!1545$  to  $\sim\!1645$  exactly coincident with the rise and fall of silver mining and metallurgy at and near Potosí in modern Bolivia. While Pb emissions undoubtedly resulted from Pb and other precious and base metal mining and ore processing, Pb often is found in silver ores; Pb pollution records have been used widely as proxies of new silver

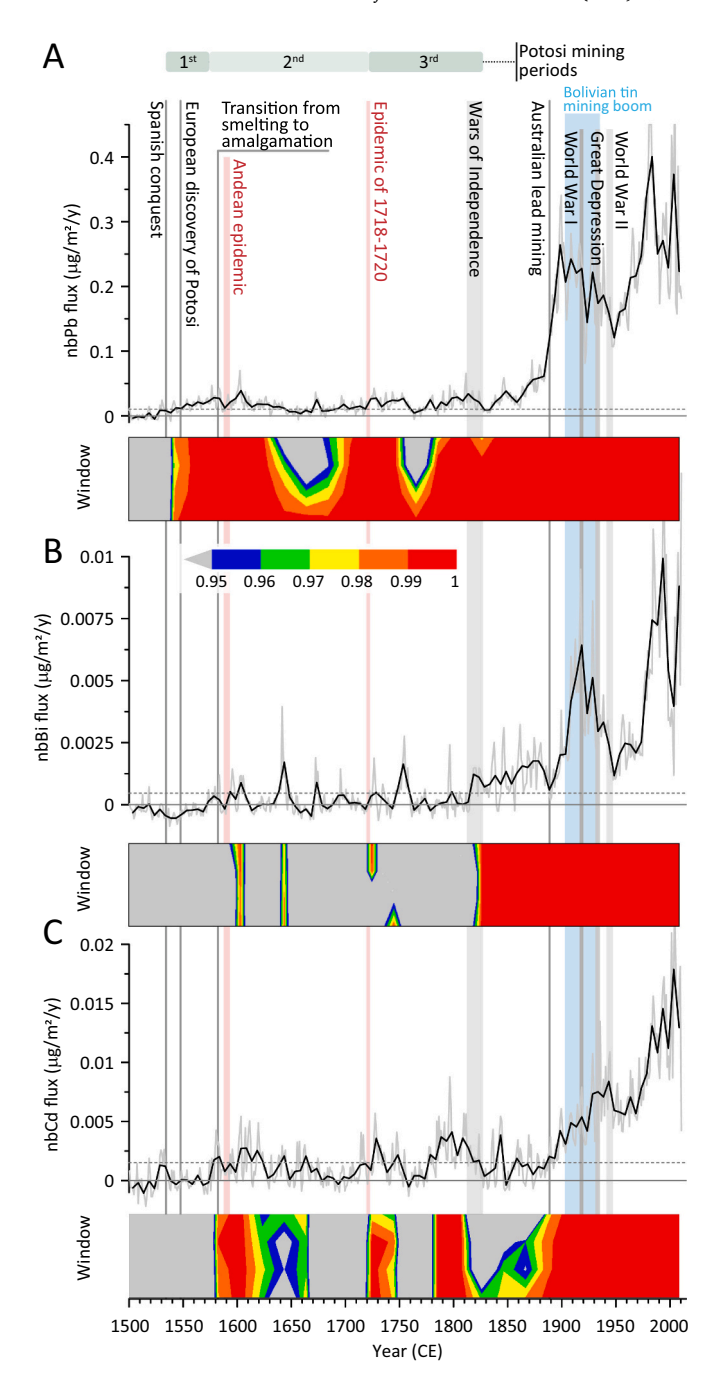


**Fig. 2.** Heavy metal pollution in East Antarctica between 1500 and 2010. Annual (light) and 5-y (heavy) non-background fluxes of (a) Pb, (b) Bi, and (c), Cd. Dotted line shows 2 s.d. variability during the 1 to 400 calibration period. Color bars show probability that fluxes over 3- to 21-y averaging windows represent periods of pollution. Only probabilities >95 % (2 s.d.) are shown in color. Also shown are selected periods and events in Andean and Australian history.

production prior to the late 18th-century Industrial Revolution and pervasive fossil fuel burning (Patterson, 1972). The Potosí region was the primary source of new silver production during this period, accounting for 48 % and 31 % of production in the Americas and globally between 1550 and 1640, respectively, while production in the larger region of upper Peru (modern Bolivia) including Potosí accounted for 53 % and 35 % (TePaske, 2010). The introduction of amalgamation at Potosí in the early 1570s greatly increased silver production without at least initially changing nbPb (Fig. 3), although metal-rich dust emissions

from the large stamping mills required to crush the ore in preparation for separation through amalgamation probably were substantial (Brown, 2012). Proximal lake sediment records from near Potosí (Cooke et al., 2008) suggest that atmospheric Pb emissions were relatively low during the 15th and early 16th centuries and increased in the late 16th century to a peak in the early 17th century consistent with the East Antarctic ice records (Supplementary Fig. 5). The only decline to near background levels in East Antarctic Pb pollution prior to  $\sim\!1630$  occurred from  $\sim\!1585$  to  $\sim\!1591$ , coeval with major recurrent epidemics, perhaps smallpox and measles, that afflicted people in the Andean region (Dobyns, 1963). This short-lived Pb pollution decline also coincided with a sharp, short-term decline in silver production registered by the

Potosí mint (TePaske, 2010) (Fig. 3). Based on FLEXPART-simulated average emission sensitivity of 0.617 ( $\mu g/m^2/y$ )/(kg/s) at the East Antarctic array, we estimate 1595 to 1605 average Pb emissions of ~1.5 kt/y from Andean mining activities assuming that the bulk of emissions were from the Potosí region and average nbPb deposition of 0.030  $\mu g/m^2/y$  in East Antarctica during this period. The estimated spatial pattern of atmospheric fallout using forward FLEXPART simulations (Fig. 4) indicates widespread Pb pollution of the Southern Hemisphere from these emissions.

The peak in East Antarctic Pb pollution during the Colonial Period occurred about 1600 and coincided with the start of a decades-long period of Cd pollution from  $\sim$ 1600 to  $\sim$ 1625, as well as a short-lived

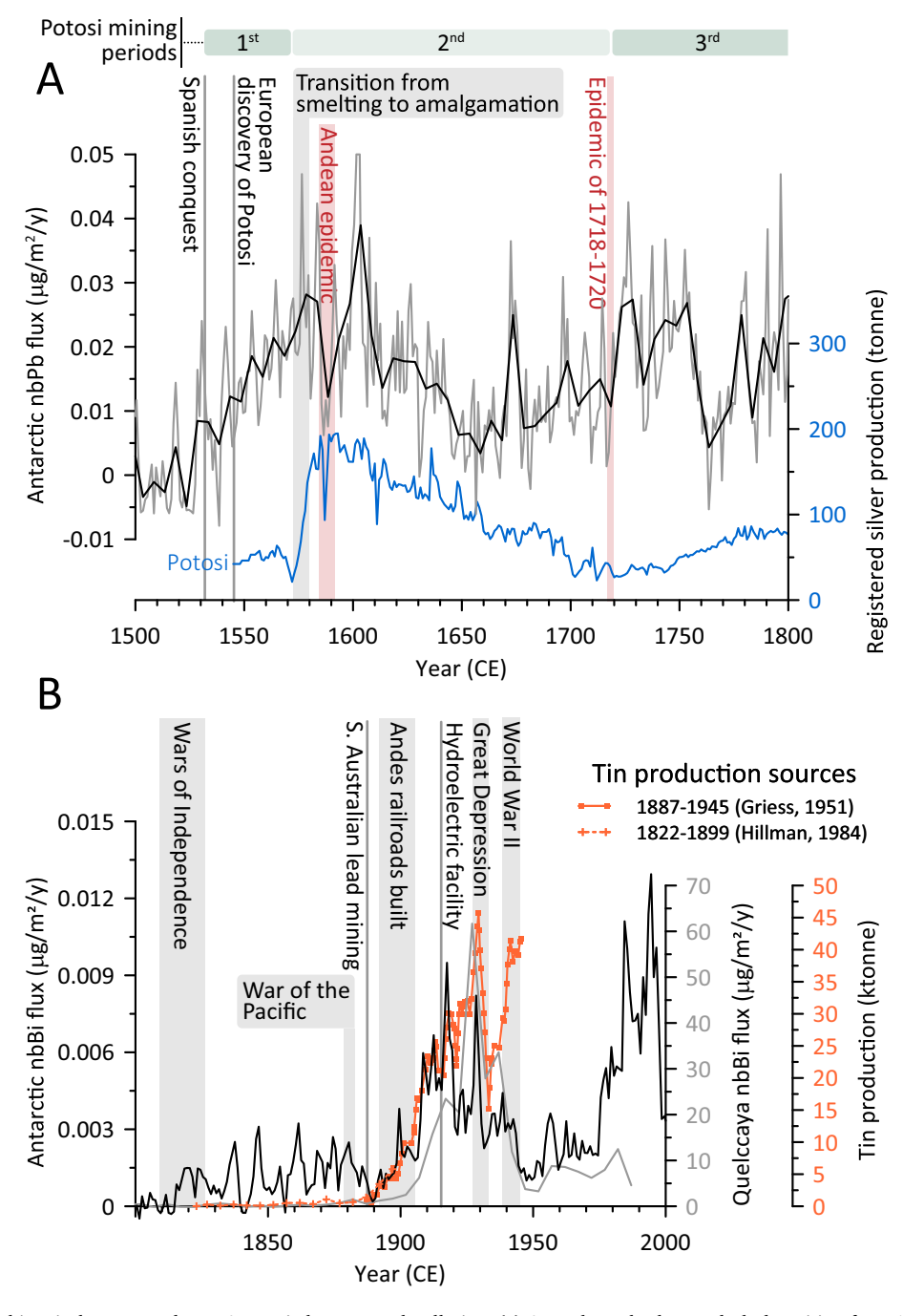
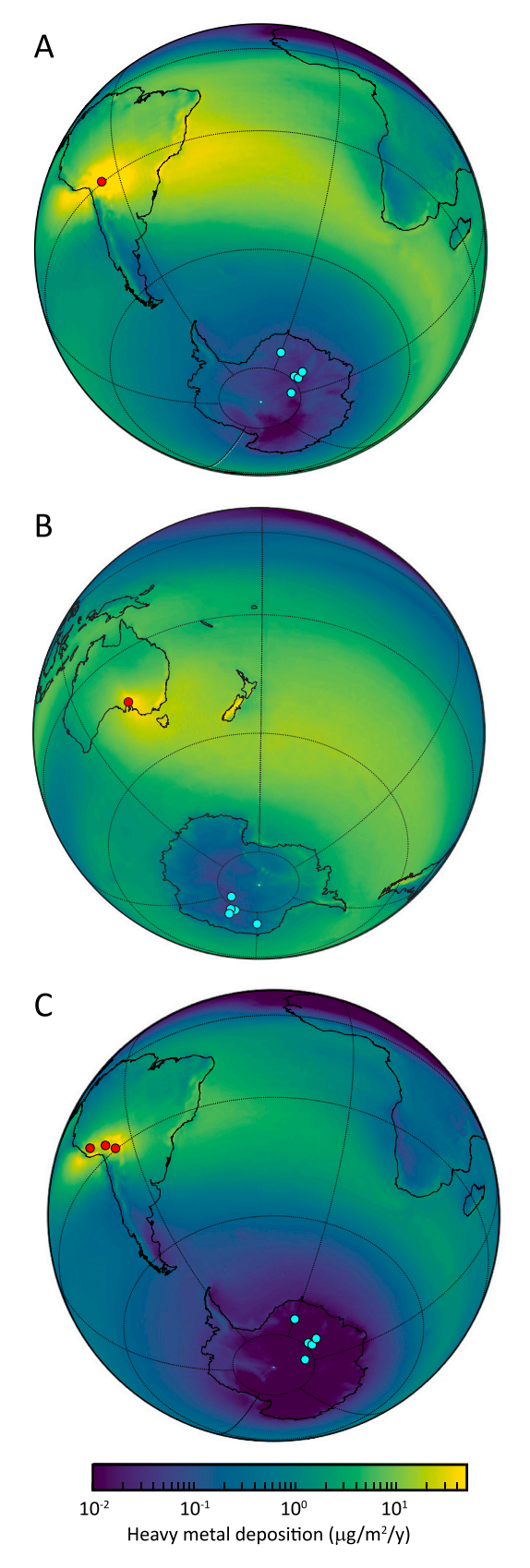


Fig. 3. Linkages between historical events and East Antarctic heavy metal pollution. (a) Annual non-background Pb deposition from 1500 to 1800 compared to annual silver production registered at the Potosí mint in modern Bolivia (TePaske, 2010). (b) Annual non-background Bi deposition from 1800 to 2000 and Bolivian tin production (Hillman, 1984; Griess, 1951). Also shown is non-background Bi deposition measured in the Qualcaya ice core from southern Peru (Uglietti et al., 2015).



(caption on next column)

Fig. 4. Estimated patterns of heavy metal pollution deposition for selected periods. (a) Average Pb pollution from 1595 to 1605 from silver, Pb, and other mining in the Potosí region of modern Bolivia. (b) Average Pb pollution in 1895 to 1905 from Pb mining at Broken Hill, Australia assuming Broken Hill emissions were the source of  $\sim\!50$  % of non-background Pb deposited in East Antarctica. (c) Average 1910 to 1920 Bi pollution from tin mining in modern Bolivia. The pattern of Pb pollution from Bolivian tin mining – probably the dominant source in Antarctica during this period based on Pb isotopic ratio variations – was similar but  $\sim\!30$  times greater than for Bi. Filled circles show locations of emission sources (red) and ice cores (cyan).

nbBi event (Fig. 2), perhaps reflecting emissions from the exploitation of new ore bodies such as the silver-sulfide-rich Oruro mines in 1606 (TePaske, 2010). Annual silver registrations (Fig. 3) were high from 1610 to 1647, but the transition from smelting to amalgamation in Oruro in 1627 may have reduced subsequent atmospheric Pb emissions. Sustained Pb pollution in East Antarctica resumed  $\sim\!1685$  and continued to the present, interrupted only by a decade-long decline from  $\sim\!1760$  to  $\sim\!1770$ . Although a sustained period of Cd pollution started just after the epidemic of 1718–1720 and lasted until  $\sim\!1750$ , the most significant period of Cd pollution in East Antarctica during the Colonial Period was from 1780 to the Wars of Independence in the early 19th century.

#### 3.6. Post-colonial and Industrial Periods: 1820s to 2010

After an initial decades-long decline to background levels following the Wars of Independence, nbPb fallout in East Antarctica increased from the 1820s to the late 1880s to reach 0.08  $\mu g/m^2/y$ . This was the highest rate of nbPb fallout during the Common Era up to that time and  $\sim 8$  times the 2 s.d. background variability during the 400-y calibration period (Fig. 2). nbPb deposition increased rapidly from the late 1880s to a maximum of  $\sim\!0.28\,\mu g/m^2/y$  in  $\sim\!1914$  before starting  $\sim\!20$ -y decline that ended during the Great Depression. Pollution Pb deposition increased sharply following WWII to an early 1980s maximum of  $\sim\!0.42\,\mu g/m^2/y$  or  $>\!40$  times the 2 s.d. background variability and was still nearly 30-fold higher than the background variability in 2010 at the end of the East Antarctic composite record.

Sustained nbBi pollution in Antarctica (Figs. 1, 2) first started in the 1820s and has persisted to present. Bi is common in Andean tin (Sn) ores, and Bolivian Sn production increased markedly first in the early 1820s, and then by an additional >10-fold by the end of the century (Hillman, 1984) in parallel with increasing nbBi deposition in Antarctica. Bolivian Sn production further increased during the early 20th century (Fig. 3) in response to strong international demand mainly from European smelters and the completion of rail lines from the Andean highlands that reduced costs to transport ores and concentrates to Pacific ports, as well as carry workers to the mining regions (Hillman, 1984). The result was a boom in Bolivian Sn mining from ~1910 to the ~1929 that ended with the onset of the Great Depression. Deposition of nbBi recorded in East and West Antarctic ice (Supplementary Fig. 6) and preserved in the Andean QND ice record (Uglietti et al., 2015) (Fig. 3) track these changes in Bolivian tin production, especially short-term variations caused by economic and political developments. nbBi deposition was within the 2 s.d. background variability at the start of the 19th century but five-fold higher a hundred years later. nbBi pollution reached a maximum >14 times the background in 1917 during the Bolivian Sn mining boom before falling to mid-19th century levels by 1950. It increased again during the second half of the 20th century, reaching a Common Era maximum in the early 1990s that was >20 times the 2 s.d. background variability (Figs. 2, 3).

Previous studies have linked the rapid increase in Antarctic Pb pollution during the late-19th century primarily to emissions from South Australia, with an associated marked decline in Pb isotopic ratios identifying the Broken Hill Pb mine and Port Pirie smelting complex as the source (McConnell et al., 2014; Vallelonga et al., 2002). Relatively constant nbPb deposition throughout Antarctica during the early 20th

century (McConnell et al., 2014) (Fig. 5; Supplementary Fig. 6) and higher <sup>206</sup>Pb/<sup>207</sup>Pb and <sup>208</sup>Pb/<sup>207</sup>Pb isotopic ratios measured at three Antarctic sites (Fig. 5), however, indicate a shift in the atmospheric emission sources affecting East Antarctica from the late 19th to the early 20th centuries. Mixing model simulations of Pb isotopic records from B54 and previously reported records from Law Dome (Vallelonga et al., 2002), and Coats Land (Planchon et al., 2003) (Fig. 5) suggest that  $\sim$ 70 to 80 % of the nbPb fallout at the Law Dome and Coats Land sites and  $\sim$ 60 % at the East Antarctic B54 site was from Port Pirie during the late 19th century (Fig. 5). By 1910, emissions from Bolivian tin production probably were dominant, accounting for  $\sim\!60$  to 75 % of the nbPb fallout over Antarctica. These findings are generally consistent with a FLEXPART-based evaluation of relative deposition sensitivities around Antarctica (Supplementary Fig. 7) showing that compared to the East Antarctic sites, the Law Dome and Coats Land sites are 2 to 5 times more sensitive to more southerly Port Pirie emissions than to those from the Bolivian tin mining region. Increased industrial emissions around the Southern Hemisphere after the 1930s, as well as widespread use of leaded gasoline starting in the 1940s with the source of the additive often being isotopically distinct Port Pirie Pb, limited attribution of potential emission sources after the mid-1930s.

FLEXPART-simulated average emission sensitivity is 3.51 and 0.515 ( $\mu g/m^2/y)/(kg/s)$  at the East Antarctic array for Port Pirie and the Bolivian tin mining region, respectively. Using the average nbPb deposition of 0.230  $\mu g/m^2/y$  during this period, we estimate 1895 to 1905 average Pb emissions of  $\sim\!1.0$  kt/y from Port Pirie and  $\sim\!7.0$  kt/y from the tin mining region (Fig. 4). By the mid-1910s, we estimate Bolivian Pb emissions of  $\sim\!11$  kt/y. Estimated Pb emissions using the Quelccaya ice record for this period also were  $\sim\!11$  kt/y based on an average nbPb deposition rate of 465  $\mu g/m^2/y$  (Uglietti et al., 2015) and a FLEXPART-simulated emission sensitivity of 1230 ( $\mu g/m^2/y)/(kg/s)$ .

Using the same average emission sensitivity of  $0.515~(\mu g/m^2/y)/(kg/s)$  and average nbBi deposition of  $0.0056~\mu g/m^2/y$  from 1910 to 1920, we estimate average Bi emissions of  $\sim 0.34~kt/y$  from the Bolivian tin mining region (Fig. 4). For the much more proximal QND record, we estimate average Bi emissions of  $\sim 0.45~kt/y$  using a FLEXPART-simulated emission sensitivity of 1230  $(\mu g/m^2/y)/(kg/s)$  and an average nbBi deposition rate of 17.5  $\mu g/m^2/y$  (Fig. 3) (Uglietti et al., 2015). The similarities in the proximal and distal emission estimates for both Pb and Bi imply a high degree of confidence in the Antarctic heavy metal records and modeling. These estimated nbBi emissions compare to an average Bolivian tin production of  $\sim 25~kt/y$  during this period (Griess, 1951), indicating an effective atmospheric Bi/Sn emission factor from Andean tin production of  $\sim 0.018$ .

A sharp, sustained drop in Cd pollution and a small, short-lived drop in Pb pollution in East Antarctica coincided with the end of the Wars of Independence. Mining infrastructure was damaged during the wars and international investments in Andean mining declined following Independence (Brown, 2012). Pb pollution increased synchronously and significantly in the late 1880s (Fig. 2) throughout Antarctica (McConnell et al., 2014) (Supplementary Fig. 5) and coincided with the start of sustained nbCd pollution in East Antarctica (Fig. 2) similar to large increases in lake sediment proxy records of local Pb and Cd contamination near Port Pirie in South Australia (Lent et al., 1992). nbCd deposition was within the 2 s.d. background variability during the mid-19th century but increased steadily to the early 1940s when nbCd deposition was five-fold higher. After a mid-20th century dip, nbCd pollution rose to a maximum in the early 20th century that was >10 times higher than the background (Fig. 2).

### 4. Conclusions

These first detailed, 2000-year records of nbPb, nbBi, and nbCd deposition from the East Antarctic ice core array and atmospheric aerosol modeling suggest that emissions from mining and metallurgy resulted in order-of-magnitude increases in hemispheric-scale heavy

metal deposition throughout much of the Southern Hemisphere. Lead pollution started as early as the 13th century during the Late Intermediate Period in the Andes and was pervasive during the Spanish Colonial period, while contamination levels for all three of these metals increased by more than an order of magnitude during the industrial period (Figs. 1, 2)

Our interpretation of the Antarctic heavy metal pollution records is based largely on detailed atmospheric aerosol modeling and comparisons to historical records such as annual Spanish Colonial silver registrations at the Potosí mint, as well as local ice and lake sediment proxy records of heavy metal pollution near postulated emission sources; such comparisons to historical records are possible only because of reliable and accurate dating of the Antarctic ice cores. While these comparisons show generally good agreement (Fig. 3, Supplementary Fig. 4), our interpretation is based on two assumptions during the Common Era: (1) long-range atmospheric transport from midlatitude aerosol sources to East Antarctica has been relatively constant so variations in Antarctic non-background heavy metals reflect only emission changes, and (2) both the metal to Ce ratios in dust and the non-crustal metal to ncTl ratios in largely quiescent volcanic fallout were similar to those during the 1 to 400 CE calibration period. Variations in black carbon aerosol deposition over East Antarctica have been linked previously to changes in the Southern Annual Mode (SAM) (McConnell et al., 2021) - the dominant mode of Southern Hemisphere atmospheric circulation variability - particularly during the past millennium for which a robust SAM reconstruction is available (Abram et al., 2014). These deposition variations were attributed primarily to meteorologically modulated biomass burning emission changes linked to the SAM rather than long-range atmospheric transport changes (McConnell et al., 2021). A direct indicator of dust and volcanic fallout provenance measured at decadal to multi-decadal resolution in pre-Spanish Colonial Antarctic ice is needed to fully evaluate these assumptions. Latitudinal Pb-isotopic variations in southern South American background aerosols have been used to investigate provenance of dust extracted from ocean sediment cores and infer past changes in large scale atmospheric circulation (Pichat et al., 2014), suggesting that detailed Pb isotopic records developed from Antarctic ice may be appropriate for such evaluations. Similar ratios in background quiescent volcanic emissions and Andean ores (Fig. 5) may limit unambiguous identification of aerosol provenance.

Comparison to Pb pollution documented in Arctic ice cores (Fig. 6) reflects the large differences in industrial development between the two hemispheres, with relative Pb increases in the Arctic ~20 times larger than those in Antarctica during the Common Era and starting thousands of years earlier (McConnell et al., 2018). Even so, both the Arctic and Antarctic ice records suggest that heavy metal pollution varied not only from discovery, exploitation, and exhaustion of new ore deposits such as Rio Tinto in the southern Iberian Peninsula and Potosí in the Andes, but also in response to plagues, local and worldwide wars and economic trends, as well as technological advancements such as amalgamation. For example, Arctic ice core records clearly show widespread, marked declines in Northern Hemisphere Pb pollution following 165 CE and 1348 CE coincident with outbreaks of the Antonine Plague and Black Death, respectively (McConnell et al., 2018; McConnell et al., 2019), while the East Antarctic records (Figs. 3, 6) show a marked decline in Southern Hemisphere Pb pollution following 1585 CE coincident with the Andean Epidemic Period (Dobyns, 1963). For perspective, the estimated Pb emissions (Fig. 4) of ~1.2 kt/y from early Andean mining and metallurgy during the Late Intermediate Period and ~ 1.5 kt/y from Potosí at the beginning of the 17th century were comparable to the similarly estimated  $\sim$ 1.1 kt/y from Iberia during the 1st-century apex of the Roman Empire (McConnell et al., 2018; McConnell et al., 2019). Estimated Pb emissions during the Bolivian tin mining boom of the early 20th century were ~10 fold higher.

Supplementary data to this article can be found online at https://doi.org/10.1016/j.scitotenv.2023.169431.

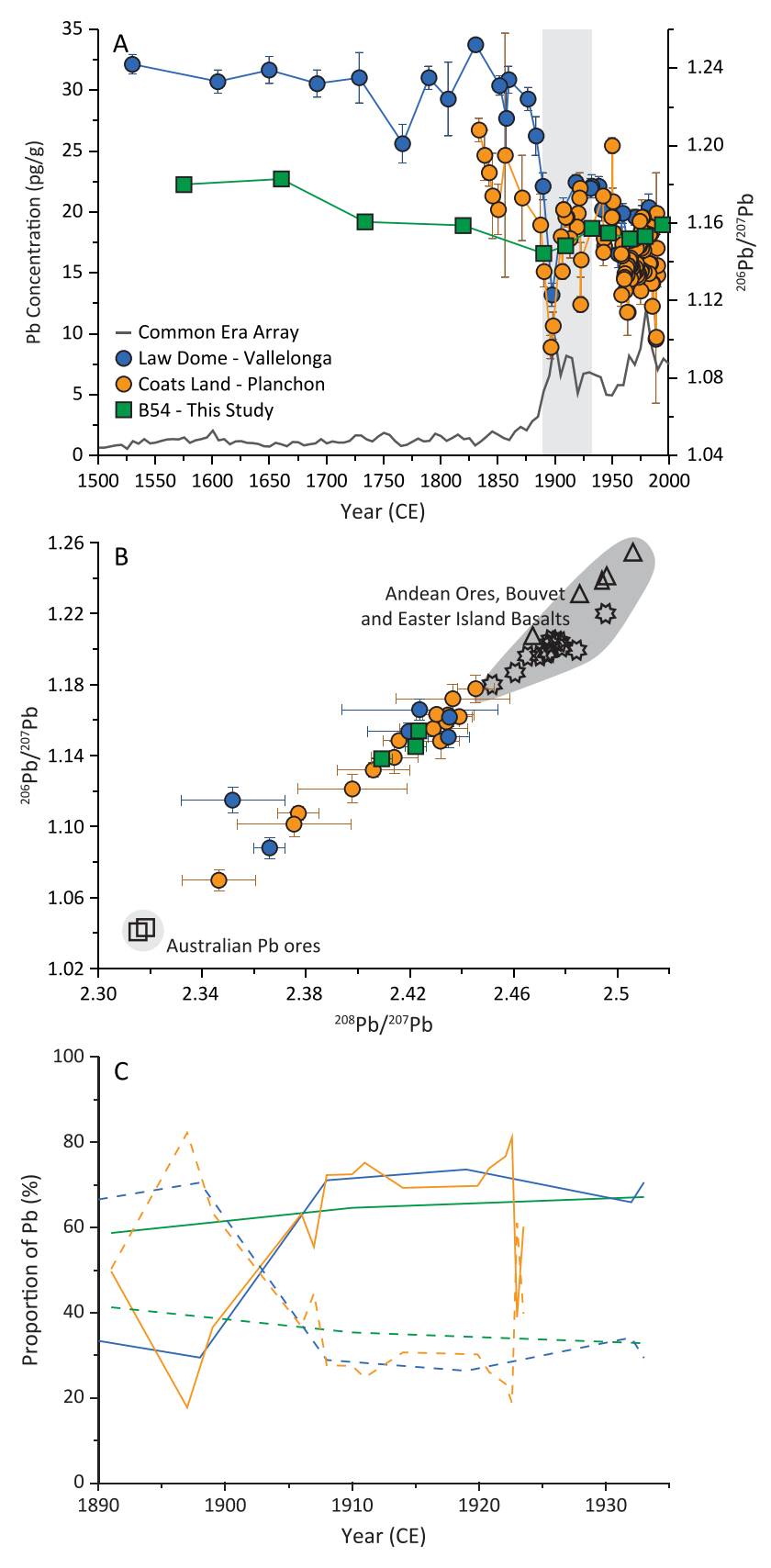


**Fig. 5.** Attribution of late-19th to early-20th century Pb pollution sources based on Pb isotopic measurements. (a) Pb concentration in the East Antarctic Common Era array and  $^{206}\text{Pb}/^{207}\text{Pb}$  ratios measured at three Antarctic sites: B54, Law Dome (Vallelonga et al., 2002), and Coats Land (Planchon et al., 2003). (b) Three-isotope plot of measurements and potential source signatures. (c) MixSIAR (Stock et al., 2018) Bayesian mixing model results indicating a shift in Pb pollution sources. Solid and dashed lines represent the proportion of Pb attributed to Andean ores and volcanism, and to Australian ores, respectively. Error bars on Pb isotope measurements show 2 s.d. uncertainty but are smaller than the symbol for B54.

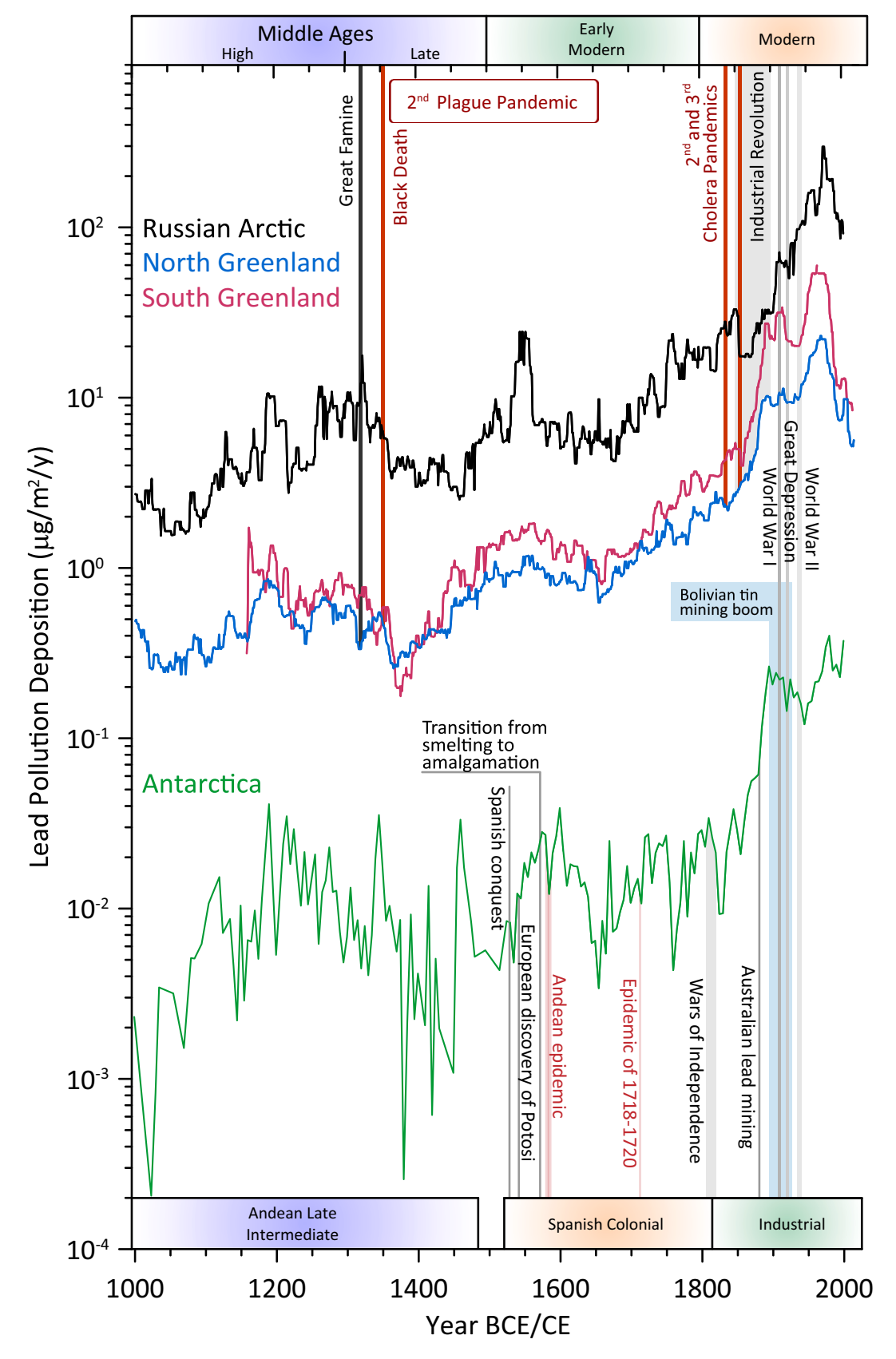


Fig. 6. Lead pollution in the polar regions during the second millennium. Shown are the East Antarctic and previously published Arctic records (McConnell et al., 2019), along with selected historical events to provide context for variations in lead pollution.

#### CRediT authorship contribution statement

Joseph R. McConnell: Conceptualization, Data curation, Formal analysis, Funding acquisition, Investigation, Methodology, Project administration, Resources, Supervision, Writing - original draft, Writing - review & editing. Nathan J. Chellman: Formal analysis, Investigation, Methodology, Software, Visualization, Writing – review & editing. Sophia M. Wensman: Formal analysis, Investigation, Methodology, Software, Visualization, Writing - review & editing. Andreas Plach: Data curation, Formal analysis, Investigation, Software, Writing - review & editing. Charles Stanish: Conceptualization, Writing - original draft. Pamela A. Santibáñez: Investigation, Writing – review & editing. Sandra O. Brugger: Investigation, Writing – review & editing. Sabine Eckhardt: Investigation, Software, Writing - review & editing. Johannes Freitag: Resources, Writing - review & editing. Sepp Kipfstuhl: Resources, Writing - review & editing. Andreas Stohl: Conceptualization, Methodology, Resources, Software, Supervision, Writing original draft, Writing - review & editing.

#### Declaration of competing interest

The authors declare that they have no known competing financial interests or personal relationships that could have appeared to influence the work reported in this paper.

Data availabilityComposite high-resolution ice core records presented in this study are provided in Supplementary Dataset 1. The individual ice core records are available upon request. FLEXPART model simulation results are in Supplementary Dataset 2. The FLEXPART model used in this study is available at https://www.flexpart.eu/. The MixSIAR model is available at https://cran.r-project.org/.

Composite high-resolution ice core records presented in this study are provided in Supplementary Dataset 1. The individual ice core records are available upon request. FLEXPART model simulation results are in Supplementary Dataset 2. The FLEXPART model used in this study is available at <a href="https://www.flexpart.eu/">https://www.flexpart.eu/</a>. The MixSIAR model is available at <a href="https://cran.r-project.org/">https://cran.r-project.org/</a>.

#### Acknowledgements

The National Science Foundation grants 0538416, 0968391, 1702830, and 1925417 to J.R.M. supported this research. We thank all Norwegian, American, and German field teams for their efforts to collect the ice cores used in this study, P. Gabrielli for providing Quelccaya ice core records, C. Cooke for providing Lake Lobato sediment records including an updated chronology, as well as students and staff in the DRI ice core group for assistance in the laboratory.

#### References

- Abram, N.J., Mulvaney, R., Vimeux, F., Phipps, S.J., Turner, J., England, M.H., 2014. Evolution of the southern annular mode during the past millennium. Nat. Clim. Chang. 4 (7), 564–569. https://doi.org/10.1038/nclimate2235.
- Barbante, C., Boutron, C.F., Morel, C., Ferrari, C., Jaffrezo, J.L., Cozzi, G., Cescon, P., 2003. Seasonal variations of heavy metals in central Greenland snow deposited from 1991 to 1995. J. Environ. Monit. 5 (2), 328–335. https://doi.org/10.1039/ b210460a.
- Bindler, R., 2006. Mired in the past looking to the future: geochemistry of peat and the analysis of past environmental changes. Glob. Planet. Chang. 53, 2009–2221. https://doi.org/10.1016/j.gloplacha.2006.03.004.
- Bowen, H., 1979. Environmental Chemistry of the Elements. Academic Press.Brown, K.W., 2012. A History of Mining in Latin America: From the Colonial Era to the Present. University of New Mexico Press.
- Candelone, J.P., Hong, S.M., Pellone, C., Boutron, C.F., 1995. Post-Industrial Revolution changes in large-scale atmospheric pollution of the Northern Hemisphere by heavy metals as documented in central Greenland snow and ice [article]. J. Geophys. Res.-Atmos. 100 (D8), 16605–16616. https://doi.org/10.1029/95JD00989.

- Cooke, C.A., Bindler, R., 2015. Lake sediment records of preindustrial metal pollution. In: Blais, J.M., Rosen, M.R., Smol, J.P. (Eds.), Environmental Contaminants: Using Natural Archives to Track Sources and Long-term Trends of Pollution. Springer, Netherlands, pp. 101–119. https://doi.org/10.1007/978-94-017-9541-8 6.
- Cooke, C.A., Abbott, M.B., Wolfe, A.P., 2008. Late-Holocene atmospheric lead deposition in the Peruvian and Bolivian Andes. The Holocene 18 (2), 353–359. https://doi.org/ 10.1177/0959683607085134
- Criscitiello, A.S., Geldsetzer, T., Rhodes, R.H., Arienzo, M., McConnell, J., Chellman, N., Marshall, S., 2021. Marine aerosol records of Arctic sea-ice and Polynya variability from New Ellesmere and Devon Island Firn Cores, Nunavut, Canada. J. Geophys. Res. Oceans 126 (9), e2021JC017205. https://doi.org/10.1029/2021JC017205.
- Dobyns, H.F., 1963. An outline of Andean epidemic history to 1720. Bull. Hist. Med. 37
- Eckhardt, S., Cassiani, M., Evangeliou, N., Sollum, E., Pisso, I., Stohl, A., 2017. Source-receptor matrix calculation for deposited mass with the Lagrangian particle dispersion model FLEXPART v10.2 in backward mode. Geophys. Model. Dev. 10, 4605–4618. https://doi.org/10.5194/gmd-10-4605-2017.
- Edmonds, M., Mather, T.A., Liu, E.J., 2018. A distinct metal fingerprint in arc volcanic emissions. Nat. Geosci. 11 (10), 790–794. https://doi.org/10.1038/s41561-018-0214-5
- Eichler, A., Gramlich, G., Kellerhals, T., Tobler, L., Schwikowski, M., 2015. Pb pollution from leaded gasoline in South America in the context of a 2000-year metallurgical history. Sci. Adv. 1 (2), e1400196 https://doi.org/10.1126/sciadv.1400196.
- Gabrielli, P., Wegner, A., Petit, J.R., Delmonte, B., De Deckker, P., Gaspari, V., Barbante, C., 2010. A major glacial-interglacial change in aeolian dust composition inferred from rare earth elements in Antarctic ice. Quat. Sci. Rev. 29 (1), 265–273. https://doi.org/10.1016/j.quascirev.2009.09.002.
- Griess, P.R., 1951. The Bolivian tin industry. Econ. Geogr. 27 (3), 238–250. https://doi. org/10.2307/141097.
- Hersbach, H., Bell, B., Berrisford, P., Hirahara, S., Horányi, A., Muñoz-Sabater, J., Thépaut, J.-N., 2020. The ERA5 global reanalysis. Q. J. R. Meteorol. Soc. 146 (730), 1999–2049. https://doi.org/10.1002/gi.3803.
- Hillman, J., 1984. The emergence of the tin industry in Bolivia. J. Lat. Am. Stud. 16 (2), 403–437. https://doi.org/10.1017/S0022216X00007124.
- Hinkley, T.K., Lamothe, P.J., Wilson, S.A., Finnegan, D.L., Gerlach, T.M., 1999. Metal emissions from Kilauea, and a suggested revision of the estimated worldwide metal output by quiescent degassing of volcanoes. Earth Planet. Sci. Lett. 170 (3), 315–325. https://doi.org/10.1016/s0012-821x(99)00103-x.
- Hong, S., Soyol-Erdene, T.-O., Hwang, H.J., Hong, S.B., Hur, S.D., Motoyama, H., 2012. Evidence of global-scale As, Mo, Sb, and Tl atmospheric pollution in the Antarctic snow. Environ. Sci. Technol. 46 (21), 11550–11557. https://doi.org/10.1021/ es20.3866.
- Hong, S.M., Candelone, J.P., Patterson, C.C., Boutron, C.F., 1994. Greenland ice evidence of hemispheric lead pollution 2-millennia ago by Greek and Roman civilizations [article]. Science 265 (5180), 1841–1843. https://doi.org/10.1126/ science.265.5180.1841.
- Hur, S.D., Soyol-Erdene, T.-O., Hwang, H.J., Han, C., Gabrielli, P., Barbante, C., Hong, S., 2013. Climate-related variations in atmospheric Sb and Tl in the EPICA Dome C ice (East Antarctica) during the past 800,000 years. Glob. Biogeochem. Cycles 27 (3), 930–940. https://doi.org/10.1002/gbc.20079.
- Legrand, M., McConnell, J.R., Preunkert, S., Bergametti, G., Chellman, N.J., Desboeufs, K., Eckhardt, S., 2022. Thallium pollution in Europe over the twentieth century recorded in alpine ice: contributions from coal burning and cement production. Geophys. Res. Lett. 49 (13), e2022GL098688 https://doi.org/10.1029/ 2022GL098688
- Lent, R.M., Herczeg, A.L., Welch, S., Lyons, W.B., 1992. The history of metal pollution near a lead smelter in Spencer gulf, South Australia. Toxicol. Environ. Chem. 36 (3–4), 139–153. https://doi.org/10.1080/02772249209357837.
- Liu, P., Kaplan, J.O., Mickley, L.J., Li, Y., Chellman, N.J., Arienzo, M.M., McConnell, J.R., 2021. Improved estimates of preindustrial biomass burning reduce the magnitude of aerosol climate forcing in the Southern Hemisphere. Sci. Adv. 7 (22), eabc1379. https://doi.org/10.1126/sciady.abc1379.
- Liu, Y., Hou, S., Hong, S., Hur, S.D., Lee, K., Wang, Y., 2011. High-resolution trace element records of an ice core from the eastern Tien Shan, central Asia, since 1953 AD. J. Geophys. Res. 116 (D12), D12307. https://doi.org/10.1029/2010JD015191.
- Longman, J., Veres, D., Ersek, V., Phillips, D.L., Chauvel, C., Tamas, C.G., 2018.
  Quantitative assessment of Pb sources in isotopic mixtures using a Bayesian mixing model. Sci. Rep. 8 (1), 6154. https://doi.org/10.1038/s41598-018-24474-0.
- Mason, E., Edmonds, M., McConnell, J.R., 2022. Volatile trace metals deposited in ice as soluble volcanic aerosols during the 17.7 ka eruptions of Mt Takahe, West Antarctic Rift. Front. Earth Sci. 10-2022 https://doi.org/10.3389/feart.2022.1002366.
- Matsumoto, A., Hinkley, T.K., 2001. Trace metal suites in Antarctic pre-industrial ice are consistent with emissions from quiescent degassing of volcanoes worldwide. Earth Planet. Sci. Lett. 186 (1) https://doi.org/10.1016/s0012-821x(01)00228-x.
- McConnell, J., Wilson, A., Stohl, A., Arienzo, M., Chellman, N., Eckhardt, S., Steffensen, J., 2018. Lead pollution recorded in Greenland ice indicates European emissions tracked plagues, wars, and imperial expansion during antiquity [article]. Proc. Natl. Acad. Sci. U. S. A. 115 (22), 5726–5731. https://doi.org/10.1073/pnas.1721818115.
- McConnell, J.R., Edwards, R., 2008. Coal burning leaves toxic heavy metal legacy in the Arctic. Proc. Natl. Acad. Sci. U. S. A. 105 (34), 12140–12144. https://doi.org/ 10.1073/pnas.0803564105.
- McConnell, J.R., Lamorey, G.W., Hutterli, M.A., 2002a. A 250-year high-resolution record of Pb flux and crustal enrichment in central Greenland. Geophys. Res. Lett. 29 (23) https://doi.org/10.1029/2002GL016016, 45-41-45-44.

- McConnell, J.R., Lamorey, G.W., Lambert, S.W., Taylor, K.C., 2002b. Continuous ice-core chemical analyses using inductively coupled plasma mass spectrometry. Environ. Sci. Technol. 36 (1), 7–11. https://doi.org/10.1021/es011088z.
- McConnell, J.R., Aristarain, A.J., Banta, J.R., Edwards, P.R., Simoes, J.C., 2007. 20th-Century doubling in dust archived in an Antarctic Peninsula ice core parallels climate change and desertification in South America. Proc. Natl. Acad. Sci. U. S. A. 104 (14), 5743–5748. https://doi.org/10.1073/pnas.0607657104.
- McConnell, J.R., Maselli, O.J., Sigl, M., Vallelonga, P., Neumann, T., Anschutz, H., Thomas, E.R., 2014. Antarctic-wide array of high-resolution ice core records reveals pervasive lead pollution began in 1889 and persists today. Sci. Rep. 4 https://doi. org/10.1038/srep05848.
- McConnell, J.R., Burke, A., Dunbar, N.W., Köhler, P., Thomas, J.L., Arienzo, M.M., Winckler, G., 2017. Synchronous volcanic eruptions and abrupt climate change ~17.7 ka plausibly linked by stratospheric ozone depletion. Proc. Natl. Acad. Sci. 114 (38), 10035–10040. https://doi.org/10.1073/pnas.1705595114.
- McConnell, J.R., Chellman, N.J., Wilson, A.I., Stohl, A., Arienzo, M.M., Eckhardt, S., Steffensen, J.-P., 2019. Pervasive Arctic lead pollution suggests substantial growth in medieval silver production modulated by plague, climate, and conflict [article]. Proc. Natl. Acad. Sci. U. S. A. 116 (30), 14910–14915. https://doi.org/10.1073/pnas.1904515116.
- McConnell, J.R., Chellman, N.J., Mulvaney, R., Eckhardt, S., Stohl, A., Plunkett, G., Aristarain, A.J., 2021. Hemispheric black carbon increase after the 13th-century Māori arrival in New Zealand. Nature 598 (7879), 82–85. https://doi.org/10.1038/ s41586-021-03858-9.
- Nriagu, J.O., 1983. Lead and Lead Poisoning in Antiquity. Wiley.
- O'Hare, P., Mekhaldi, F., Adolphi, F., Raisbeck, G., Aldahan, A., Anderberg, E., Team, A., 2019. Multiradionuclide evidence for an extreme solar proton event around 2,610 BP (similar to 660 BC) [article]. Proc. Natl. Acad. Sci. U. S. A. 116 (13), 5961–5966. https://doi.org/10.1073/pnas.1815725116.
- Patterson, C.C., 1972. Silver stocks and losses in ancient and medieval times. Econ. Hist. Rev. 25, 205–233. https://doi.org/10.1111/j.1468-0289.1972.tb02173.x.
- Pichat, S., Abouchami, W., Galer, S.J.G., 2014. Lead isotopes in the Eastern Equatorial Pacific record Quaternary migration of the South Westerlies. Earth Planet. Sci. Lett. 388, 293–305. https://doi.org/10.1016/j.epsl.2013.11.035.
- Pisso, I., Sollum, E., Grythe, H., Kristiansen, N.I., Cassiani, M., Eckhardt, S., Stohl, A., 2019. The Lagrangian particle dispersion model FLEXPART version 10.4. Geosci. Model Dev. 12 (12), 4955–4997. https://doi.org/10.5194/gmd-12-4955-2019.
- Planchon, F.A.M., van de Velde, K., Rosman, K.J.R., Wolff, E.W., Ferrari, C.P., Boutron, C.F., 2003. One hundred fifty-year record of lead isotopes in Antarctic snow from Coats Land. Geochim. Cosmochim. Acta 67 (4), 693–708. https://doi.org/ 10.1016/s0016-7037(00)01136-5.
- Rosman, K.J.R., Chisholm, W., Boutron, C.F., Candelone, J.P., Hong, S., 1994. Isotopic evidence to account for changes in the concentration of lead in Greenland snow between 1960 and 1988. Geochim. Cosmochim. Acta 58 (15), 3265–3269. https://doi.org/10.1016/0016-7037(94)90054-X.
- Sangster, D.F., Outridge, P.M., Davis, W.J., 2000. Stable lead isotope characteristics of lead ore deposits of environmental significance. Environ. Rev. 8 (2), 115–147. https://doi.org/10.1139/a00-008.

- Schultze, C.A., Stanish, C., Scott, D.A., Rehren, T., Kuehner, S., Feathers, J.K., 2009. Direct evidence of 1,900 years of indigenous silver production in the Lake Titicaca Basin of Southern Peru. Proc. Natl. Acad. Sci. 106 (41), 17280. https://doi.org/ 10.1073/pnas.0907733106
- Shotyk, W., Weiss, D., Appleby, P., Cheburkin, A., Frei, R., Gloor, M., Van der Knaap, W., 1998. History of atmospheric lead deposition since 12,370 C-14 yr BP from a peat bog, Jura Mountains, Switzerland [article]. Science 281 (5383), 1635–1640. https:// doi.org/10.1126/science.281.5383.1635.
- Sigl, M., McConnell, J.R., Toohey, M., Curran, M., Das, S.B., Edwards, R., Severi, M., 2014. Insights from Antarctica on volcanic forcing during the Common Era. Nat. Clim. Chang. 4, 693–697. https://doi.org/10.1038/NCLIMATE2293.
- Sigl, M., Winstrup, M., McConnell, J., Welten, K., Plunkett, G., Ludlow, F., Woodruff, T., 2015. Timing and climate forcing of volcanic eruptions for the past 2,500 years. Nature 523, 543–549. https://doi.org/10.1038/nature14565.
- Stock, B.C., Jackson, A.L., Ward, E.J., Parnell, A.C., Phillips, D.L., Semmens, B.X., 2018. Analyzing mixing systems using a new generation of Bayesian tracer mixing models. PeerJ 6. https://doi.org/10.7717/peerj.5096.
- Sun, S.S., 1980. Lead isotopic study of young volcanic rocks from mid-ocean ridges, ocean islands and island arcs. Philos. Trans. R. Soc. Lond. A 297 (1431), 409–445.
   TePaske, J.J., 2010. A New World of Gold and Silver. Brill.
- Uglietti, C., Gabrielli, P., Cooke, C.A., Vallelonga, P., Thompson, L.G., 2015. Widespread pollution of the South American atmosphere predates the industrial revolution by 240 y. Proc. Natl. Acad. Sci. 112 (8), 2349. https://doi.org/10.1073/ pnas.1421119112.
- Vallelonga, P., Van de Velde, K., Candelone, J.P., Morgan, V.I., Boutron, C.F., Rosman, K. J.R., 2002. The lead pollution history of Law Dome, Antarctica, from isotopic measurements on ice cores: 1500 AD to 1989 AD. Earth Planet. Sci. Lett. 204 (1–2), 291–306. Article Pii s0012-821x(02)00983-4. https://doi.org/10.1016/s0012-821x(02)00983-4.
- Vallelonga, P., Gabrielli, P., Balliana, E., Wegner, A., Delmonte, B., Turetta, C., Barbante, C., 2010. Lead isotopic compositions in the EPICA Dome C ice core and Southern Hemisphere potential source areas. Quat. Sci. Rev. 29 (1), 247–255. https://doi.org/10.1016/j.quascirev.2009.06.019.
- Van de Velde, K., Vallelonga, P., Candelone, J.P., Rosman, K.J.R., Gaspari, V., Cozzi, G., Boutron, C.F., 2005. Pb isotope record over one century in snow from Victoria Land, Antarctica. Earth Planet. Sci. Lett. 232 (1–2), 95–108. https://doi.org/10.1016/j.epsl.2005.01.007.
- Weis, D., Kieffer, B., Maerschalk, C., Barling, J., de Jong, J., Williams, G.A., Mahoney, J. B., 2006. High-precision isotopic characterization of USGS reference materials by TIMS and MC-ICP-MS. Geochem. Geophys. Geosyst. 7 (8) https://doi.org/10.1029/2006GC001283 n&#x2F:a-n&#x2F:a.
- Wensman, S.M., Shiel, A.E., McConnell, J.R., 2022. Lead isotopic fingerprinting of 250-years of industrial era pollution in Greenland ice. Anthropocene 38, 100340. https://doi.org/10.1016/j.ancene.2022.100340.
- Wolff, E.W., Suttie, E.D., 1994. Antarctic snow record of Southern-Hemisphere lead pollution. Geophys. Res. Lett. 21 (9), 781–784. https://doi.org/10.1029/94gl00656.